Low-energy electron-collision processes in molecular chlorine

T. N. Rescigno
Physical Science Directorate, Lawrence Livermore National Laboratory, P.O. Box 808, Livermore, California 94550
(Received 6 December 1993)

The results of close-coupling calculations using the complex Kohn variational method are reported for a variety of low-energy electron-collision processes involving molecular chlorine. We report cross sections for elastic scattering and momentum transfer, as well as dissociative excitation of the five lowest electronically excited states ($^{1,3}\Pi_u$, $^{1,3}\Pi_g$, $^3\Sigma_u^+$) which are formed by promoting an occupied valence electron into an antibonding ($5\sigma_u$) orbital. We also report cross sections for the excitation of the lowest bound optically allowed states in Cl_2. The cross sections, especially at very low energies, are found to depend sensitively on both target polarization and a proper balance of correlation effects in the N- and $(N+1)$-electron systems. Comparison is made between the results of this study and the limited body of experimental results available for this system.

PACS number(s): 34.80.Gs

I. INTRODUCTION

A major obstacle to the optimization of industrially important plasma processes through numerical modeling is the lack of reliable cross sections, either calculated or measured, for electron collisions with reactive gases [1]. The measurement of such cross sections is extremely difficult and the number of molecules for which a comprehensive set of cross sections is available is surprisingly small [2]. The theoretical calculation of such cross sections is also a challenging task, but several *ab initio* methods have been developed in recent years [3–5], which are capable of providing useful electron-molecule collision cross sections, not only for elastic scattering, but for electronic excitation and dissociation as well. Such calculations are complicated and computationally demanding and the field is still developing. Because of the potential usefulness of computational approaches in providing electron-scattering cross sections for molecules used in a variety of plasma applications, it is important that we be able to assess the reliability of the various approaches presently available and to develop a knowledge of the sensitivity of calculated cross sections to the approximations that must inevitably be made in the various formulations. Such knowledge can only be developed as the number of molecules for which detailed comparison between theory and experiment increases.

Chlorine gas is widely used in the plasma etching of semiconductors. In such applications, chlorine molecules are dissociated in a discharge and the Cl atoms efficiently etch a silicon substrate [6]. Very few direct measurements of electron-Cl_2 scattering cross sections have been carried out. Cross sections for ionization and dissociative electron attachment were measured during the 1970s [7] and there has been a recent experimental study of electron-impact dissociation [8]. Cross sections for other dominant electron-collision processes have been derived from Boltzmann analysis and early swarm measurements [9]. To our knowledge, no previous theoretical studies of electron-Cl_2 scattering have been reported.

The purpose of this paper is to present the results of a fairly comprehensive study of low-energy electron-Cl_2 scattering. We have calculated cross sections for elastic scattering and momentum transfer, as well as dissociation through excitation of all the electronically excited states ($^{1,3}\Pi_u$, $^{1,3}\Pi_g$, $^3\Sigma_u$) which are formed by promoting an occupied valence electron into the lowest, antibonding ($5\sigma_u$) orbital. We have also calculated cross sections for excitation of the lowest bound optically allowed states of Cl_2. The calculations were carried out using the complex Kohn variational technique [3] which has proven to be a reliable tool for the study of elastic and electronically inelastic electron-molecule scattering. Cl_2 is an attaching gas and consequently the cross sections, particularly at very low energies, are found to depend sensitively on a proper balance of electron correlation in the N- and $(N+1)$-electron systems. It is hoped that the present study will prove useful to those interested in chlorine plasmas and that it will provide an impetus for further experimental work which is sorely needed for this important system.

II. THEORY

The complex Kohn method is a variational technique which imposes outgoing-wave boundary conditions through the use of a trial wave function built from both square-integrable (Cartesian Gaussian) and continuum basis functions. The method has been developed in a series of articles over the past few years [3,10–13] and so only a brief review will be given here. The T matrix is characterized as the stationary point of the functional

$$[T]=T-2\int\Psi(H-E)\Psi\ . \tag{1}$$

The stationary point $\delta[T]=0$ is found by varying the linear parameters C, D, and T of a trial wave function of the form

$$\Psi_{\Gamma_0 K_0} = \sum_{\Gamma c} A(\Phi_\Gamma \otimes \phi_c) C_{\Gamma c} + \sum_{c'} \Theta_{c'} D_{c'} + J_{\Gamma_0 K_0} + \sum_{\Gamma K} T_{\Gamma_0 K_0 \Gamma K} H^+_{\Gamma K} , \quad (2)$$

where A is the antisymmetrizer, Φ_Γ is an energetically open N-electron target state, ϕ_c is a one-electron square-integrable basis function, and the direct product symbol implies strong orthogonality between Φ_Γ and ϕ_c. $\Theta_{c'}$ is an $(N+1)$-electron configuration state function (CSF) built from square-integrable functions and is orthogonal to $A(\Phi_\Gamma \otimes \phi_c)$. The terms $J_{\Gamma_0 K_0}$ and $H^+_{\Gamma K}$ incorporate the asymptotic behavior into the trial function. Their structure is identical to $A(\Phi_\Gamma \otimes \phi_c)$ except that ϕ_c is replaced, respectively, by one-particle regular and outgoing-wave continuum basis functions. The coefficients $T_{\Gamma_0 K_0 \Gamma K}$ are elements of the T matrix labeled by target state quantum numbers Γ and the angular momentum quantum numbers $K \equiv (lm)$ of the scattered electron. The symbols Γ_0, K_0 indicate the initial state of the system.

The Kohn method is based on a Hamiltonian formulation of the scattering problem. This feature, along with the particular form of the trial function used, makes it possible to use the tools of modern electronic-structure theory in a straightforward manner to calculate many of the required matrix elements, even when correlated target states are included in the expansion. Many of the computational details related to this part of the formulation have been given elsewhere [11]. The explicit appearance of continuum (free) functions in the trial wave function leads to bound-free and free-free integrals which are not normally encountered in electronic-structure calculations. Two approximations are adopted which eliminate the need to compute many of the bound-free and free-free matrix elements. The separable exchange approximation [14] assumes that the exchange portions of the Hamiltonian, being relatively short ranged, can be well represented by projecting them onto a finite basis of square-integrable CSF's. Because of the othogonality condition imposed on the basis functions,

$$\langle J_{\Gamma_0 K_0} | A(\Phi_\Gamma \otimes \phi_c) \rangle = 0 , \quad (3)$$

it follows that all bound-free and free-free exchange matrix elements vanish [15]. Similarly, matrix elements involving free functions and $(N+1)$-electron function CSF's Θ are made to vanish by the same technique:

$$\langle J_{\Gamma K} | (H-E) | \Theta \rangle \approx \sum_c \langle J_{\Gamma K} | A(\Phi_\Gamma \otimes \phi_c) \rangle \times \langle A(\Phi_\Gamma \otimes \phi_c) | (H-E) | \Theta \rangle = 0 . \quad (4)$$

It is important to note that the disappearance of the above continuum matrix elements is not just a consequence of the orthogonality of the bound and continuum orbitals, but also the *assumption* that the exchange and optical potential operators can be accurately represented by a separable expansion in terms of the bound molecular orbitals. This latter assumption is of course an approximation; whether or not it is a good approximation depends upon how many functions we include in the underlying L^2 basis and how close it comes to being complete for the purpose of representing the operators in question [15]. It has been our experience that good convergence can be obtained with these techniques except at *extremely* low energies. Nevertheless, to minimize errors associated with the reliance on separable expansions, the basis sets we employ are much larger that what is typically employed in an electronic structure calculation. In this connection, we have also begun to explore alternative integral technology [16] which removes the reliance on primitive separable expansions and allows the use of much smaller basis sets, but we have yet to fully implement this technology.

The approximation schemes just mentioned are not justified for the long-range direct interactions. The direct bound-free and free-free integrals can be reduced to three-dimensional numerical quadrature by using one-particle reduced density operators to construct the direct potentials [10]. Three-dimensional quadrature of the integrals typically required in molecular problems are difficult to converge because the integrands are dominated by cusps at the atomic nuclei. We developed an adaptive three-dimensional (3D) quadrature technique some time ago [10] to address this problem which we used in all previous applications of the complex Kohn method. Recently, we have been made aware of a multicenter numerical integration scheme originally proposed by Becke [17], which is based on the idea of decomposing a single molecular integral into a sum of one-center, atomiclike integrations and which is currently being used in applications of density-functional theory [18]. We have adapted this technique to the evaluation of the continuum integrals required here and find that we can now achieve substantially more accurate results (six decimal place accuracy is readily achievable) with fewer than half the number of quadrature points required in our original scheme. Moreover, we have also been able to speed up the evaluation of the required direct potentials considerably by using numerical schemes based on this type of quadrature. Analytic evaluation of the direct potentials on a 3D grid [10], while requiring only one-electron Coulomb integrals that are a standard part of any molecular structure code, can be time consuming, especially for large molecules. We will defer further discussion of these numerical developments to a separate study.

The trial function given in Eq. (2) is quite general and can be used to incorporate correlation and polarization effects into the formulation [11]. The $(N+1)$-electron CSF's $\Theta_{c'}$ used in $\Psi_{\Gamma_0 K_0}$ are generally of two distinct types. The first class consists of "penetration" terms and serves to relax any constraints implied by requiring the free functions to be orthogonal to the set of orbitals used to built the open-channel target states. These CSF's can be generated by constructing the direct product of a target molecular orbital and the N-electron configurations used in generating the target wave functions, retaining all resulting terms consistent with the Pauli exclusion principle and employing them in fixed linear combinations dictated by the expansion coefficients of the various open-

channel target states. When multiconfiguration target states are employed, this procedure, which is common to many close-coupling treatments, can, as we have previously demonstrated in our study of e^-+F_2 scattering [13], lead to unphysical effects at intermediate energies, where no structure is expected, unless *all* energetically open target states that can be generated from the list of N-electron configurations used to build the Φ_Γ are explicitly included in the open-channel part of $\Psi_{\Gamma_0 K_0}$. Of course, this may be neither possible nor desirable in general. For this reason, it is prudent to seek as compact a description of the target states as possible. Another simple expedient is to retain in the trial wave function only those penetration terms corresponding to the dominant configuration for each open-channel target state corresponding to the dominant configuration for each open-channel target state included, assuming of course that a compact representation can be found in which each target state is dominated by a single configuration [19].

A second class of $(N+1)$-electron CSF's is used to introduce correlation and polarization effects into the trial wave function which are not included in the open-channel part of the expansion. The inclusion of such effects is especially important at collision energies of several electron volts or less where dynamical distortion of the target by the incident electron can have a substantial effect on the computed cross sections. In introducing such terms, however, some care must be taken to treat correlation effects in the N- and $(N+1)$-electron systems in a balanced fashion; this is particularly important in a system like e^-+Cl_2 which possesses a stable negative ion. Ultimately, the partitioning of terms between the open- and closed-channel spaces and the appropriateness of including certain terms is dictated by physical considerations. In this spirit, we have used different types of approximate trial wave functions depending on the process being considered, the symmetry under consideration, and the collision energy involved. In formulating these various approximations, we have relied heavily on our experience with earlier calculations on similar systems, particularly low-energy e^-+F_2 [13] and e^-+Li_2 scattering [20].

III. BASIS SETS AND TARGET STATES

All calculations in this study were carried out at the experimental equilibrium internuclear distance, $3.758a_0$ [21]. The basis sets used in the various calculations are summarized in Table I. The target states were determined using a $6s5p$ contraction of the $12s9p$ Cl basis given by McLean [22]. This basis was augmented with an additional Rydberg p function and two d functions. The ground-state self-consistent field (SCF) energy in this basis is $-918.980\,747$ hartrees. For the scattering calculations, the target basis was augmented with two d functions on the chlorine atoms and four s and three p functions at the bond center. This basis is also listed in Table I.

Peyerimhoff and Buenker [23] have reported the results of a large-scale configuration-interaction study of the electronic states of Cl_2. Near its equilibrium geometry, the $X\,^1\Sigma_g^+$ ground state of Cl_2 is nominally described by the configuration $(\text{core})5\sigma_g^2 2\pi_u^4 2\pi_g^4$. We are using (core) to denote all the inner-shell orbitals. The lowest excited states ($^3\Pi_u$, $^1\Pi_u$, $^3\Pi_g$, $^1\Pi_g$, and $^3\Sigma_u^+$) are formed by promoting an electron from one of the three valence orbitals into an occupied $5\sigma_u$ orbital, which is essentially the antibonding combination of the $3p_z$ orbitals. These states (apart from the $^3\Pi_u$ state which has a shallow minimum near $4.5a_0$) are all strictly dissociative. The lowest excited states with a significant dissociation energy are the optically allowed Rydberg ($2\pi_g \rightarrow 4p\sigma, 4p\pi$) $^1\Pi_u$ and $^1\Sigma_u^+$ states with excitation energies of ~ 9.5 eV. The Cl_2^- ion is bound in $^2\Sigma_u^+$ symmetry and crosses the neutral Cl_2 curve, i.e., becomes electronically autodetaching, at a slightly shorter internuclear distance. The Cl_2^- ion is nominally described by the configuration $(\text{core})5\sigma_g^2 2\pi_u^4 2\pi_g^4 5\sigma_u$.

We have carried out scattering calculations at various

TABLE I. Gaussian basis sets used in target and scattering calculations.

Center	Type	Exponent	Coefficient[a]
		Target basis	
Chlorine	s	105 818.8	0.000 743
Chlorine	s	15 872.0	0.005 753
Chlorine	s	3 619.7	0.029 676
Chlorine	s	1 030.8	0.118 010
Chlorine	s	339.91	0.365 230
Chlorine	s	124.538	0.581 221
Chlorine	s	124.538	0.137 548
Chlorine	s	49.514	0.622 881
Chlorine	s	20.806	0.290 143
Chlorine	s	6.4648	1.0
Chlorine	s	2.5254	1.0
Chlorine	s	0.5378	1.0
Chlorine	s	0.1935	1.0
Chlorine	p	589.78	0.002 760
Chlorine	p	139.85	0.021 536
Chlorine	p	44.795	0.095 916
Chlorine	p	16.612	0.262 315
Chlorine	p	6.599	0.726 811
Chlorine	p	6.5995	−1.564 924
Chlorine	p	2.7141	1.495 778 1
Chlorine	p	0.9528	1.0
Chlorine	p	0.3580	1.0
Chlorine	p	0.1250	1.0
Chlorine	p	0.05	1.0
Chlorine	d	0.7	1.0
Chlorine	d	0.25	1.0
		Supplemental scattering basis	
Bond center	s	0.1	1.0
Bond center	s	0.04	1.0
Bond center	s	0.016	1.0
Bond center	s	0.0064	1.0
Bond center	p	0.025	1.0
Bond center	p	0.015	1.0
Bond center	p	0.008	1.0
Chlorine	d	1.5	1.0
Chlorine	d	0.1	1.0

[a]Underlines separate contracted basis functions.

levels of approximation using both single-configuration and correlated target states. The correlated target state wave functions were obtained from single and double-excitation configuration-interaction (CI) calculations in which the core orbitals were held doubly occupied. This produces expansions of several thousand terms, which are not practical for use in scattering calculations. In order to obtain a more compact description of the relevant target states, two different sets of natural orbitals were extracted from these calculations. One set consisted of the natural orbitals obtained by diagonalizing the ground-state density matrix. From this orbital set, we retained a "vital" set consisting of the orbitals strongly occupied in the ground state plus the $5\sigma_u$ orbital and a "virtual" set comprised of an additional π_u and σ_g orbital. The ground state was then described by a valence CI in which no more than one electron was allowed to occupy a virtual orbital. A similar prescription was used in generating CSF's to describe the negative ion. These calculations give a ground-state wave function with an energy of $-919.013\,582$ hartrees and a positive electron affinity of 1.2 eV. Calculations of low-energy scattering using this basis will be reported below.

A second set of natural orbitals was obtained by averaging the density matrices of the ground and low-lying dissociative states. From this set we retained only the core and valence ($5\sigma_g$, $2\pi_u$, $2\pi_g$, and $5\sigma_u$) orbitals. Calculations including all distributions in which the ten outer electrons are allowed to occupy these valence orbitals produce a set of excited states whose excitation energies are given in Table II. For comparison, we also list the vertical excitation energies obtained by Buenker and Peyerimhoff [23]. These target states were used in calculating cross sections for dissociation.

The optically allowed Rydberg states were only treated at the single-configuration level, using simple improved virtual orbitals (IVO's). We obtained excitation energies for the $^1\Pi_u$ and $^1\Sigma_u^+$ states of 10.84 and 10.96 eV, respectively, compared to the values of 9.22 and 9.32 eV reported by Peyerimhoff and Buenker.

We have also carried out calculations at the polarized-SCF level. For those calculations, the ground state was treated at the Hartree-Fock level and (closed) excited states were described by singly exciting the target into a minimal set of polarized orbitals obtained in a subspace orthogonal to the occupied orbitals. There are a number of different techniques available for calculating polarized orbitals. Details of the procedure we use have been given elsewhere [12]. The value of the polarizability of Cl_2 we obtained at this level was $30.76a_0$, which compares favorably with the extrapolated experimental value of $30.35a_0$ given by Oddershede and Svendsen [24].

TABLE II. Vertical electronic energies (in eV) from the ground state of Cl_2 to low-lying dissociative states.

State	This work	Peyerimhoff and Buenker[a]
$X\,^1\Sigma_g^+$	0.0	0.0
$1\,^3\Pi_u$	3.36	3.31
$1\,^1\Pi_u$	4.30	4.05
$1\,^3\Pi_g$	6.38	6.29
$1\,^1\Pi_g$	7.01	6.83
$1\,^3\Sigma_u^+$	7.02	6.87

[a]From Ref. [22].

IV. RESULTS

A. Low-energy elastic scattering

For scattering in the range from 0.2 to 3.5 eV, we performed calculations in $^2\Sigma_g^+$, $^2\Sigma_u^+$ and $^2\Pi_u$ symmetry and included continuum functions up to $l=6$ in the trial function. Higher-symmetry components do not contribute significantly at these energies. Our calculated elastic and momentum-transfer cross sections in the energy region below the first excited triplet state are shown in Figs. 1 and 2, respectively.

Cross sections in this energy range are sensitive to several effects which are not properly described at the static-exchange level. The static-exchange approximation, in which the target is treated at the SCF level and closed-channel effects are ignored, gives cross sections that are dominated by a shape resonance near 0.5 eV. This behavior can be traced to the $^2\Sigma_u^+$-symmetry component, reflecting the fact that Cl_2^- is unbound at this level of treatment. To remedy this shortcoming, we carried out correlated target calculations with the ground-state natural orbital set described above, using the electron distributions given in Table III to generate the Kohn trial function. The first two distributions generate both the open-channel portion of the trial function, consisting of the direct product of a scattering orbital and the correlated ground-state function described in the previous section, as well as closed-channel contributions arising from the complement of target states that are generated from the target natural orbitals. The third distribution generates penetration terms, where all electrons occupy natural orbitals, which are needed to relax orthogonality constraints on the total wave function. The fourth distribution completes this set and also generates the dominant configuration for the Cl_2^- ion. We see from Figs. 1 and 2 that cross sections computed at this level do not show the

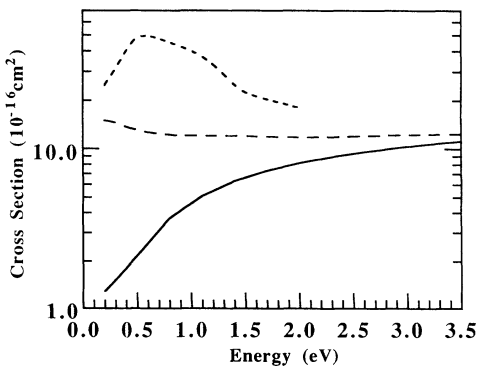

FIG. 1. Low-energy $e^- + Cl_2$ elastic cross sections at three different levels of approximation: long-dashed line, static-exchange approximation; short-dashed line, correlated-target calculation; solid line, correlated-target plus polarized SCF for $^2\Sigma_g$ symmetry component.

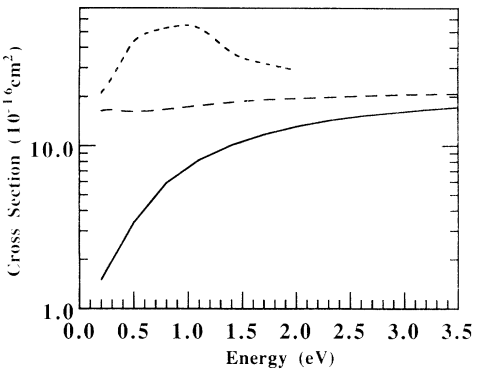

FIG. 2. As in Fig. 1, for momentum-transfer cross section.

TABLE IV. Electron distributions used to generate the $^2\Sigma_g$ component of the low-energy Kohn trial wave function in the polarized-SCF approximation.

Core orbitals[a]	Occupied orbitals[b]	Polarized orbitals	Scattering orbitals[c]
24	10	0	1
24	9	1	1
24	10	1	0
24	9	2	0

[a]Refers to the 12 inner-shell SCF orbitals that are held doubly occupied.
[b]The set consists of the $5\sigma_g$, $2\pi_u$, and $2\pi_g$ SCF orbitals.
[c]The set contains the entire complementary set of orbitals formed from the target plus supplementary scattering basis.

effects of a shape resonance and are relatively flat over the energy range in question.

Although the correlated target calculations do include a limited number of closed-channel effects, they only incorporate roughly one third of the total polarizability. We would expect this deficiency to lead to an overestimation of the $^2\Sigma_g^+$ component of the low-energy cross sections. Therefore, for this symmetry component alone, we carried out a third set of calculations at the polarized-SCF level which, as we have previously stated, gives a very good representation of the target polarizability. The electron distributions included for this calculation are given in Table IV. This final set of results, which we feel to be the most accurate, are also shown in Figs. 1 and 2. To extend these calculations to higher energy, we must take explicit account of open-channel excited states in the calculation.

B. Dissociative excitation

We have carried out coupled-channel calculations of dissociative excitation over the energy range from 4.35 eV, which is just above the threshold for exciting the $^1\Pi_u$ state, to 30 eV. The calculation included contributions from total symmetry components $^2\Sigma_g^+$, $^2\Sigma_u^+$, $^2\Pi_u$, $^2\Pi_g$, $^2\Delta_g$, and $^2\Delta_u$. For these calculations, we used the set of averaged natural orbitals and used the electron distributions given in Table V to build the Kohn trial function. From the first distribution, we only retained terms corresponding to the direct product of a scattering orbital and either the ground- or low-lying dissociative excited states previously described. These terms are explicitly included as part of the open-channel portion of the Kohn trial function or as correlation terms Θ_c when the relevant target state is energetically closed. By explicitly including all these target states in the trial wave function (ten channels, including both components of the doubly degenerate Π and Δ states), we account for coupling between the excited target states. As we have shown in other studies [25], neglecting these couplings can lead to significant redistribution of excitation probability among the states in question. The second distribution generates penetration terms, precisely one of each of the symmetries $^2\Sigma_g^+$, $^2\Sigma_u^+$, $^2\Pi_u$ and $^2\Pi_g$, which relaxes the orthogonality constraints between the excited target states and the corresponding channel scattering functions. With this prescription, there are no inconsistencies between the open- and closed-channel parts of the total wave function and no spurious resonance structures are encountered.

In Fig. 3, we plot the total cross sections for excitation of each of the low-lying states, along with the total dissociation cross section. In Fig. 4 we show a comparison between our calculated total cross section and the experi-

TABLE III. Electron distributions used to generate low-energy, correlated target Kohn trial wave function.

Core orbitals[a]	Vital orbitals[b]	Virtual orbitals[c]	Scattering orbitals[d]
24	10	0	1
24	9	1	1
24	10	1	0
24	11	0	0

[a]Refers to the 12 inner-shell SCF orbitals that are held doubly occupied.
[b]The set consists of the $5\sigma_g$, $2\pi_u$, $2\pi_g$, and $5\sigma_u$ ground-state natural orbitals.
[c]This set contains a correlating π_u and σ_g natural orbital.
[d]The set contains the entire complementary set of orbitals formed from the target plus supplementary scattering basis.

TABLE V. Electron distributions used to generate the Kohn trial wave function for dissociative excitation.

Core orbitals[a]	Vital orbitals[b]	Scattering orbitals[c]
24	10	1
24	11	0

[a]Refers to the 12 inner-shell SCF orbitals that are held doubly occupied.
[b]The set consists of the $5\sigma_g$, $2\pi_u$, $2\pi_g$, and $5\sigma_u$ averaged natural orbitals.
[c]The set contains the entire complementary set of orbitals formed from the target plus supplementary scattering basis.

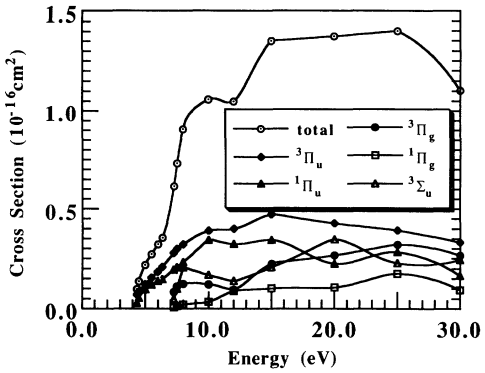

FIG. 3. Calculated $e^- + Cl_2$ dissociation cross sections through various low-lying electronic states.

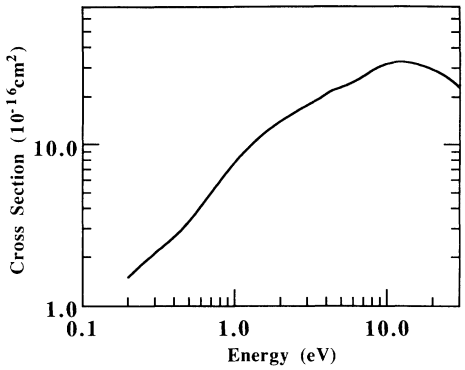

FIG. 5. Calculated total elastic-scattering cross section. See text for description of approximations used in different energy ranges.

mental values reported by Cosby [8]. Evidently, the total dissociation cross section is dominated by the contribution corresponding to excitation of the $^3\Pi_u$ state over the entire energy range considered. This is consistent with Cosby's measurements of fragment energy release which are dominated by a broad peak centered at 1 eV. (Note that the ground-state dissociation energy of Cl_2 is 2.5 eV.) However, the contribution from the other dissociative states is by no means negligible and correlates well with the peak near 5-eV fragment energy release seen by Cosby. While Cosby attributed this peak to excitation of the $^1\Pi_g$ state, our calculations show larger cross sections for exciting the $^3\Pi_g$ and $^3\Sigma_u^+$ states. However, because we have performed calculations at only one internuclear separation, we are not in a position to provide theoretical values for fragment energy distributions.

The elastic T-matrix elements obtained from the coupled-states calculations allow us to extend our values for elastic-scattering and momentum-transfer cross sections up to 30 eV. We have combined these results with those presented in the previous section and present them in Figs. 5 and 6. In Fig. 6, we also plot the momentum-transfer cross sections of Rogoff, Kramer, and Piejak [9] which were deduced from a transport analysis of early swarm measurements of a 80% He-20% Cl_2 mixture [26]. Given the uncertainties inherent in the transport analysis, we find the agreement to be very good.

C. Optically allowed states

To obtain cross sections for excitation of the optically allowed $^1\Pi_u$ and $^1\Sigma_u^+$ Rydberg states, we performed three-state calculations, coupling an SCF function for the ground state with single-configuration, IVO (improved virtual orbital) wave functions for the excited states. For this set of cross sections, we carried out variational calculations in $^2\Sigma_g^+$, $^2\Sigma_u^+$, $^2\Pi_u$, $^2\Pi_g$, and $^2\Delta_g$ symmetry and included partial waves up to $l=6$. To incorporate the effects of higher partial waves and other symmetries, which are important for optically allowed cross sections, we use a closure formula, which includes these contributions through infinite order in the first Born approximation [27]. The results are shown in Fig. 7. For comparison, we also show results given by the simple dipole-Born approximation, which are seen to significantly overestimate the cross sections. Rogoff, Kramer, and Piejak [9] have also reported cross sections for these excitations, which they treat as a single state. We compare their derived cross sections to our calculated values in Fig. 8. Once again, we find reasonable agreement.

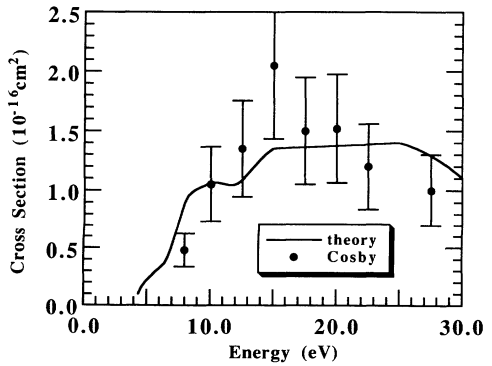

FIG. 4. Comparison of calculated total dissociation cross section and experimental measurements of Cosby [8].

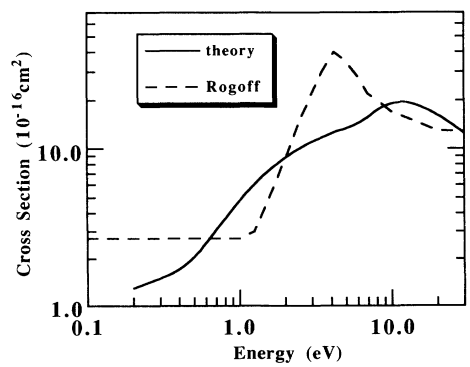

FIG. 6. Comparison of calculated momentum-transfer cross section and values deduced by Rogoff, Kramer, and Piejak [9].

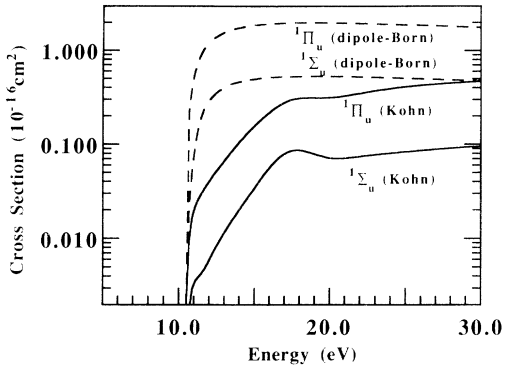

FIG. 7. Calculated total cross sections for excitation of the Rydberg $^1\Pi_u$ and $^1\Sigma_u$ states of Cl_2. Comparison of variational and dipole-Born results.

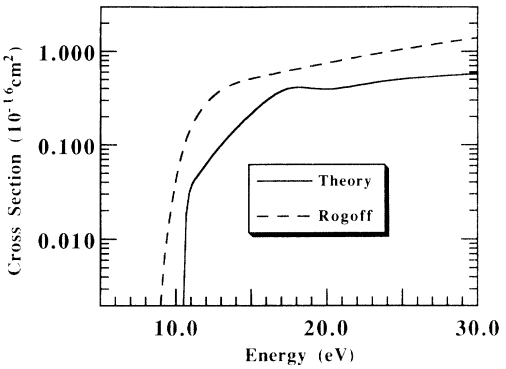

FIG. 8. Comparison of summed excitation cross sections for Rydberg $^1\Pi_u$ and $^1\Sigma_u$ states of Cl_2 and values deduced by Rogoff, Kramer, and Piejak [9].

V. SUMMARY

We have presented a set of theoretical cross sections for low-energy $e^- + Cl_2$ scattering. Over the range from zero to several eV incident electron energy, we have demonstrated that some care must be taken to incorporate the effects of electron correlation and target polarization into the scattering calculations to avoid badly overestimating the total elastic and momentum-transfer cross sections. At higher impact energies, we have calculated cross sections for electronic excitation, involving both dissociative as well as optically allowed Rydberg states. We have carried out close-coupling calculations for these cross sections and have indicated the procedures that are necessary to avoid spurious structure in the computed cross sections at intermediate energies when correlated target states are used. We have found reasonably good agreement between our calculated results and the limited body of other results available for comparison. We hope that this initial study will prompt additional experimental, as well as theoretical, work on this important system.

ACKNOWLEDGMENT

This work was performed under the auspices of the U.S. Department of Energy by the Lawrence Livermore National Laboratory under Contract No. W-7405-Eng-48.

[1] L. E. Kline and M. J. Kushner, Crit. Rev. Solid State Mater. Sci. **16**, 1 (1989).
[2] S. Trajmar, D. F. Register, and A. Chutjian, Phys. Rep. **97**, 219 (1983).
[3] B. I. Schneider and T. N. Rescigno, Phys. Rev. A **37**, 3749 (1988).
[4] K. Takatsuka and V. McKoy, Phys. Rev. A **24**, 2473 (1981); **30**, 1734 (1984).
[5] P. G. Burke, C. J. Noble, and S. Salvini, J. Phys. B **16**, L113 (1983); J. Tennyson and C. J. Noble, *ibid.* **18**, 155 (1985).
[6] D. M. Manos and D. L. Flamm, *Plasma Etching* (Academic, Boston, 1989).
[7] R. E. Cener and A. Mandl, J. Chem. Phys. **37**, 4104 (1972); M. V. Kurepa and D. S. Belic, J. Phys. B **11**, 3719 (1978).
[8] P. C. Cosby, Bull. Am. Phys. Soc. **35**, 1822 (1990); P. C. Cosby and H. Helm, Wright Laboratory Report No. WL-TR-93-2004, U.S. Air Force Material Command, Wright Patterson AFB, OH 45433-7650.
[9] G. L. Rogoff, J. M. Kramer, and R. B. Piejak, IEEE Trans. Plasma Sci. **PS-14**, 103 (1986).
[10] C. W. McCurdy and T. N. Rescigno, Phys. Rev. A **39**, 4487 (1989).
[11] A. E. Orel, T. N. Rescigno, and B. H. Lengsfield III, Phys. Rev. A **44**, 4328 (1991).
[12] B. H. Lengsfield III, T. N. Rescigno, and C. W. McCurdy, Phys. Rev. A **44**, 4296 (1991).
[13] B. H. Lengsfield III and T. N. Rescigno, Phys. Rev. A **44**, 2913 (1991).
[14] T. N. Rescigno and A. E. Orel, Phys. Rev. A **23**, 1134 (1981); **24**, 1267 (1981).
[15] T. N. Rescigno and B. I. Schneider, Phys. Rev. A **37**, 1044 (1988).
[16] C. W. McCurdy and T. N. Rescigno, Phys. Rev. A **46**, 255 (1992).
[17] A. D. Becke, J. Chem. Phys. **88**, 2547 (1988).
[18] C. W. Murray, N. C. Handy, and G. J. Laming, Mol. Phys. **78**, 997 (1993).
[19] A. E. Orel, T. N. Rescigno, and B. H. Lengfield, Phys. Rev. A **42**, 5292 (1990).
[20] T. J. Gil, C. W. McCurdy, T. N. Rescigno, and B. H. Lengsfield, Phys. Rev. A **47**, 255 (1993).
[21] K. P. Huber and G. Herzberg, *Molecular Spectra and Molecular Structure. IV. Constants of Diatomic Molecules* (Van Nostrand, New York, 1950).
[22] A. D. McLean and G. S. Chandler, J. Chem. Phys. **72**,

5639 (1980).
[23] S. D. Peyerimhoff and R. J. Buenker, Chem. Phys. **57**, 279 (1981).
[24] J. Oddershede and E. N. Svendsen, Chem. Phys. **64**, 359 (1982).
[25] S. A. Parker, C. W. McCurdy, T. N. Rescigno, and B. H. Lengsfield III, Phys. Rev. A **43**, 3514 (1991); T. J. Gil, B. H. Lengsfield, C. W. McCurdy, and T. N. Rescigno, *ibid.* **49**, 2551 (1994).
[26] V. A. Bailey and R. H. Healey, Philos. Mag. **19**, 725 (1935).
[27] T. N. Rescigno and B. I. Schneider, Phys. Rev. A **45**, 2894 (1992).